The University of Tehran Press

Pollution

Print ISSN: 2383-451X
Online ISSN: 2383-4501

https://jpoll.ut.ac.ir/

Adsorptive Removal of Crystal violet Dye Using Biochar Synthesised from Agriculture Residue: A Sustainable Study

Jyoti Chowdhry | Khush Kataria | Pradeep Khyalia | Jitender Singh Laura | Meenakshi Nandal✉

Department of Environmental Science, Maharishi Dayanand University, Rohtak-124001. Haryana, India

Article Info

Article type:
Research Article

Article history:
Received: 7 February 2025
Revised: 28 June 2025
Accepted: 12 August 2025

Keywords:
Adsorption
Monolayer adsorption
Low-cost adsorbents
Rice straw
Sugarcane bagasse

ABSTRACT

In recent years, there has been a growing interest in eliminating pollutants from aqueous solutions through adsorption onto carbonaceous materials. Rice straw biochar (RCB) and sugarcane bagasse biochar (SCB) were evaluated as adsorbents for removing crystal violet (CV) dye from aqueous solutions. pH (1–12), adsorbent dosage (0.1–0.5 g/L), CV concentration (10–50 mg/L), and contact time (30–150 min) were varied at room temperature to obtain the optimum condition. The maximum monolayer adsorption capacities of 476.2 and 161.29 mg/g for SCB and RCB, respectively were obtained at optimum condition. The adsorption equilibria fitted best to the Freundlich isotherm model (R2 = 0.9985), and the kinetics followed a pseudo-second-order model (R2 = 0.9907), indicating chemisorption and monolayer coverage. Under these conditions, Crystal violet dye removal efficiencies exceeded 90% for both biochars. These results demonstrate the high potential of RCB and SCB as low-cost bioadsorbents for effective CV dye removal in the wastewater treatment.

Cite this article: Chowdhry, J., Kataria, Kh., Khyalia, P., Singh Laura, J., & Nandal, M. (2025). Adsorptive Removal of Crystal violet Dye Using Biochar Synthesised from Agriculture Residue: A Sustainable Study. *Pollution*. 11(4), 1306-1320. https://doi.org/10.22059/poll.2025.390103.2788

DOI: https://doi.org/10.22059/poll.2025.390103.2788

INTRODUCTION

Water plays a vital role in sustaining life and supporting biological processes. However, increasing water contamination from a variety of pollutants including pesticides, synthetic dyes, heavy metals, pharmaceuticals, radioactive substances, and microbial agents poses serious risks to both human health and aquatic ecosystems (Foong et al., 2022; Sahoo et al., 2023; Khan et al., 2023). Among the contaminants, synthetic dyes, especially crystal violet (CV) is particularly hazardous (Salahudeen et al., 2020), recognized for its high toxicity, non-biodegradability, and carcinogenic potential (Abu Elella et al., 2019). Even in small concentrations, CV contributes to severe color pollution, hindering sunlight penetration in water and disrupting aquatic life (Lellis et al., 2019; Hussein et al., 2019).

Among the alternative methods, adsorption stands out due to its cost-effectiveness, high efficiency, and environmental friendliness (Rapo et al., 2020). Studies have demonstrated biochar's efficacy in dye removal, with varying adsorption capacities depending on the feedstock: peanut hull (526.31 mg/g), palm kernel shell (24.45 mg/g), banana peel (1.68 mg/g), rice husk (185.6 mg/g), and cassava bagasse (149.96 mg/g) (Khan et al., 2023; Kyi et al., 2020; Azhar-ul-Haq et al., 2024; Luyen et al., 2019; Gonçalves et al., 2024). Sugarcane bagasse

*Corresponding Author Email: *Meenakshi.env.sc@mdurohtak.ac.in*

(SCB), a fibrous residue rich in cellulose, lignin, and hemicellulose, has also gained interest due to its abundance and favorable adsorption properties. SCB contains natural polysaccharides and functional groups (carboxyl, hydroxyl, carbonyl) that promote dye adsorption via hydrogen bonding, electrostatic attraction, and chelation (Omer et al., 2022; Bhatti et al., 2021; Kumar et al., 2021). Previous studies have demonstrated the potential of rice straw biochar for dye removal, with crystal violet (CV) adsorption efficiencies reaching up to 92.70%, and magnetic composites achieving around 90% removal (Elhamid et al., 2020; Geetha et al., 2024). However, existing research is limited in scope, often examining a narrow range of dye types and overlooking essential optimization parameters. Furthermore, comprehensive studies on enhancing CV removal through biochar modification remain scarce.

Therefore, the objective of this research is to develop a cost-effective and sustainable method for removing crystal violet dye from wastewater using rice straw-derived biochar, by optimizing critical adsorption parameters and evaluating performance through isotherm, kinetic, and thermodynamic models.

MATERIALS AND METHODS

Rice straw was obtained from an agricultural field (Bohar village) and sugarcane bagasse from a sugarcane juice shop in Rohtak city.

Reagents

Sodium hydroxide (Loba Chemicals Private Limited), hydrochloric acid (HCl) (Loba Chemicals Private Limited), and crystal violet dye (CV, 99.9%, Loba Chemicals Private Limited) were used as reagents, and all solutions were prepared using distilled water. A stock solution of 1000 mg/L CV was prepared by the dissolution 1 g of dye with 1 L of distilled water in a volumetric flask. The stock solution was stored in a dark place to prevent depolarization. All solutions with the desired concentrations used in this study were prepared according to APHA (APHA,1995).

Instruments

The instruments used during the experimental investigations included a pH meter (LMMP-30, LABMAN), UV–Vis spectrophotometer (Single Beam, Model LI-296, LABMAN), Hybrid muffle furnace (Harrier HMF-1200P, Faridabad, Hry.), Hot air Oven (Biogen Scientific, Meerut U.P) analytical balance (UniBloc AUW 120D, SHIMADZU), and incubator shaker (Widsons Scientific Works, Rohtak, Hry.). Separate sets of equipment and reagents were used as required throughout the study to maintain consistency and avoid contamination.

Preparation of Bio-Adsorbent

Bagasse and rice straw was dried in sunlight and then at 70 °C for in oven. It is breakdown into tiny pieces (about 1 to 1.5 cm long) with the help of scissor, ground using a grinding machine, and then pass through a sieve with a mesh size of 1 mm to get uniform size particles of rice straw and bagasse (Chen et al.,2016). After that it was again dried for one hour at 70 ^{0}C in the oven to completely remove the moisture. Both bioadsorbent then pyrolyzed at 550 ^{0}C in a modified muffle furnance to obtain biochar.

Adsorption Experiment

The adsorption performance of RSB and SCB in solution was evaluated in the batch adsorption studies. All adsorption tests were carried out three times, and the average data was calculated. In a typical experiment, 250 mL conical flasks were filled with a predetermined quantity of adsorbents and 100 mL of CV solution. For a predetermined amount of time, the flasks were

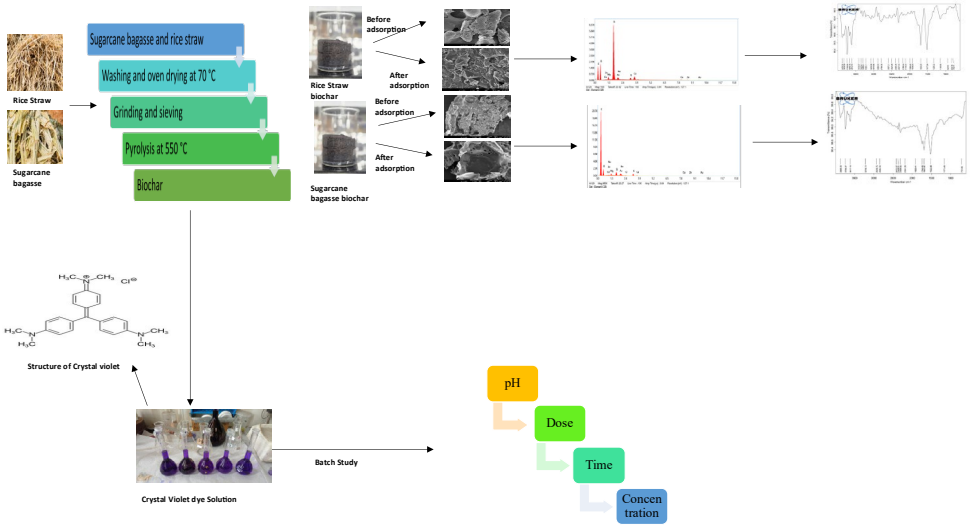

Fig. 1. Flow chart of the preparation of biochar and optimisation of parameters

shaken at 150 rpm in a Wilson Scientific Works incubator shaker at room temperature (25 ± 2 °C). Using Whatman 0.45µm filter paper, the solutions were filtered. Following filtering, UV-Vis spectroscopy was used to measure the residual CV in solution at an ideal wavelength of 590 nm, which corresponds to the maximal adsorption capacity for CV.

A number of preliminary tests were conducted with varying solution pH (1–12), adsorbent dosage (0.1–0.5 g/L), CV concentration (10–50 mg/L), and contact period (30–150 min) in order to identify the ideal experimental conditions. Further, the percentage CV removal was determined as per following equation:

$$\text{Dye removal (\%)} = \frac{C_0 - C_e}{C_0} \times 100 \quad (1)$$

where C_0 is the initial concentration and C_e is the final concentration.

Kinetic Models Study

The amount of CV adsorbed at different time intervals, q_t (mg/g), in the adsorption kinetics experiment was determined as follows:

$$q_t = \frac{C_0 - C_t}{m} \times V \quad (2)$$

where V is the volume of the solution (L), m is the mass of the biochar utilised (g), C_0 is the initial concentration of CV (mg/L), and C_t is the concentration of CV at time t (mg/L). The experimental data in this work were assessed using the pseudo-first-order, pseudo-second-order and intra-particle diffusion models. Eqs. (3), (4), and (5) present three models, respectively (Rezazadeh et al., 2021).

$$Ln\left(q_e - q_t\right) = Lnq_e - k_1 t \quad (3)$$

$$\frac{t}{q_t} = \frac{1}{k_2 \cdot q_e^2} + \frac{t}{q_e} \quad (4)$$

$$q_t = k_p t^{0.5} + C \quad (5)$$

The levels of adsorbed adsorbate at equilibrium are denoted by q_e (mg/g); the pseudo-first-order model's rate constant is k_1 (1/min); the pseudo-second-order model's response rate constant is k_2 (g/mg/min); intra-particle diffusion rate constant k_p (mg/g·min), and boundary layer thickness constant C.

Isotherm Models Study

The Langmuir model (5), the Freundlich model (6) and the Temkin model (8) were used to fit the isotherm adsorption data (Khan et al., 2023). The Langmuir model holds true when every molecule has a single layer of adsorption coverage on a completely homogeneous surface. Nevertheless, multilayer sorption and non-ideal adsorption on heterogeneous surfaces can also be addressed by the Freundlich isotherm and the Temkin isotherm considers the effects of adsorbent-adsorbate interactions and assumes that the heat of adsorption decreases linearly with coverage.

$$\frac{C_e}{q_e} = \frac{1}{q_m \cdot K_l} + \frac{C_e}{q_m} \quad (6)$$

$$Logq_e = LogK_f + \frac{1}{n} LogC_e \quad (7)$$

$$q_e = BLnK_t + BLnC_e \quad (8)$$

Where q_m (mg/g) is the maximum adsorption capacity; C_e (mg/L) is the CV concentration in the solution phase at the equilibrium time; K_f (mg/g) is the Freundlich constant represented by the sorption; n is the Freundlich exponent; K_l (L/g) is the Langmuir equilibrium constant; B (J/mol) is Temkin constant related to adsorption heat, and K_T (L/g) is Temkin isotherm equilibrium binding constant.

RESULTS AND DISCUSSION

Characterization

SEM Analysis

The sugarcane bagasse biochar SEM micrograph is displayed in Fig. 2 with before and after photos at varying magnification levels. The sugarcane's carbonisation produced holes and micropores. The activated carbon that was created had a consistent porosity structure. There is a chance that the dye will be absorbed because of the many voids on the thermally carbonised carbons' surfaces. Hazzaa et al. (2015) suggest that incomplete microsphere formation during aromatization/polymerization events is what causes the uneven shapes embedded on the surface.

Several particles that resemble microspheres are condensed on the surface as seen in Fig. 2(a). Conversely, compacted smaller microsphere forms gathered on the surface are depicted in Fig. 2(b). This study aligns with the findings of Zhao et al. (2013) by demonstrating that higher acid concentrations facilitate the formation of larger microspheres. Consistent with Jais et al. (2021), the microsphere formation is driven by the degradation of cellulose, hemicellulose, and partial lignin breakdown. Together, these findings confirm that acid-mediated biomass decomposition is essential for microsphere development.

The SEM micrographs of rice straw samples are displayed in Fig. 2. Additionally, the rice straw sample in Fig. 2(c) and 2(d) was made by pyrolysis in a muffle furnace at 550°C. This

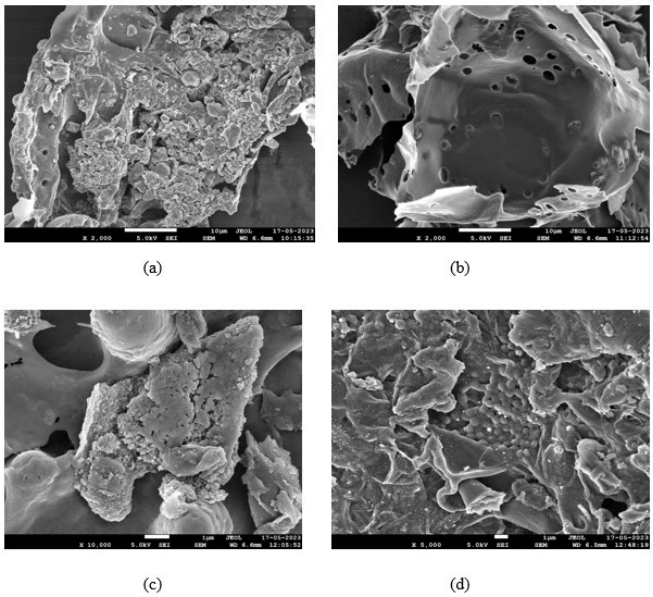

Fig. 2. SEM analysis of (a) SCB before adsorption, (b) SCB after adsorption, (c) RSB before adsorption, and (d) RSB after adsorption

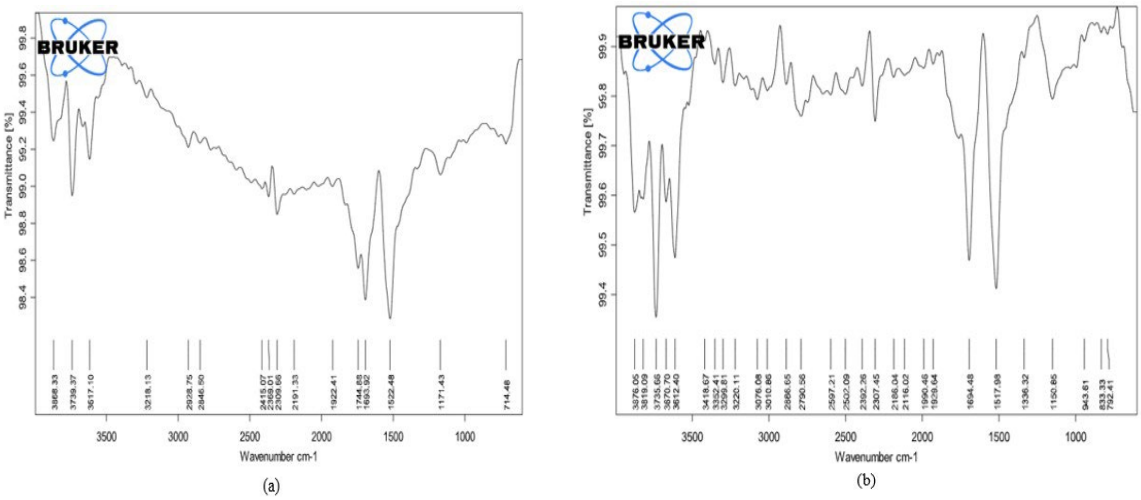

Fig. 3. FTIR analysis of (a) Sugarcane bagasse biochar and (b) Rice straw biochar

micrograph shows the presence of contaminants and pieces, which were shown in cluster form in Fig. 2(a). Peng et al. (2011) also reported on this phenomenon. Additionally, the biochar's porous structure and uneven, spherical bulges were visible in the SEM images, and these features served as efficient catalyst adsorption sites. It was determined that the biochar surface's tiny spherical bulges might be the cause of the material's increased catalytic activity. Furthermore, the majority of the macropores were discovered in the RSB, especially at the sample's open end Fig. 2(b). Since more CV can be adsorbed in the biochar, the existence of macropores in the biochar is crucial (Abd-Elhamid et al., 2020).

FTIR Analysis

The FTIR spectrum of Fig. 3 presented shows transmittance as a function of wavenumber (cm-1). Key absorption peaks include strong bands around 3400 cm-1, indicating O-H stretching typically associated with hydroxyl groups, which may originate from adsorbed moisture,

alcohols, or phenolic compounds present in the biomass structure, and around 1700 cm-1, suggesting C=O stretching from carbonyl groups. Peaks near 2900 cm-1 could be attributed to C-H stretching in alkanes. The fingerprint region (below 1500 cm-1) shows multiple peaks, indicating the presence of various functional groups and complex molecular structures. The hydroxyl groups of sugarcane bagasse will condense into alkoxide groups during thermal treatment to create biochar, lowering the quantity of surface adsorbed (Moharm et al., 2021).

Band shifting may suggest that these functional groups interact with the CV molecules. Many abrupt decreases are thought to be caused by CV species in addition to ionic interactions between the O-H groups in the structure.

The transmittance against wavenumber in the rice straw biochar FTIR spectrum (Fig. 3a and 3b) indicates the presence of several functional groups. In sugarcane bagasse biochar (Fig. 3a) presence of O-H stretching vibrations, indicative of hydroxyl groups likely stemming from water or phenolic compounds, is evidenced by the broad peak at approximately 3400 cm-1. Peaks at around 2900 cm-1 are associated with aliphatic hydrocarbons having C-H stretching, according to Zhang et al. (2018). The prominent absorption observed at about 1700 cm-1 indicates the presence of C=O stretching vibrations, potentially originating from carbonyl or carboxyl groups. Rice straw biochar (Fig. 3b) shows similar peaks, with O–H and aliphatic C–H stretches, a clear C=O stretch at 1700 cm-1, and aromatic C=C vibrations at 1600 cm-1. According to Kamal et al. (2017), the proximity of the C=C stretching bands around 1600 cm-1 suggests the existence of aromatic compounds generated during the pyrolysis process. Additionally, multiple peaks in the fingerprint region (below 1500 cm-1) imply a structurally diverse composition with various functional groups, including alcohols, ethers, and phenols exhibiting C-O stretching. These functional groups underscore the biochar's capacity for adsorption and reactivity, rendering it advantageous for environmental and agricultural applications.

Effects of parameters study

Effect of pH

Using rice straw and sugarcane bagasse biochars, the influence of pH on the percentage of crystal violet dye removed reveals that both biochars function better at higher pH levels, with sugarcane bagasse biochar showing improved overall efficiency (Fig. 3a). At acidic pH levels (2–5), the removal percentage of rice straw biochar is still very low (40–50%); however, when pH climbs to 10, it increases dramatically to almost 90%, reaching an optimal removal percentage of 91% at pH 11. The increase in adsorption at high pH is likely because the biochar surface becomes more negatively charged (deprotonation of –OH and –COOH groups) and the CV dye remains cationic, enhancing electrostatic attraction. At low pH, excess H^+ competes with CV for adsorption sites and protonates the surface, reducing dye uptake (Shamkhi & Hussein, 2022). Studies have shown similar results P. Homagai et al., in 2022 use rice-biomass chars (rice husk or straw) that typically show better CV uptake under neutral/alkaline conditions; they report >98% removal at pH 10. Sugarcane bagasse biochar, on the other hand, exhibits a higher removal efficiency of roughly 70% at lower pH levels and reaches nearly total removal (~100%) at pH values between 8 and 9. It even maintains a high level of effectiveness at pH 10, with pH 9 being the optimal removal percentage. In comparison to rice straw biochar, sugarcane bagasse biochar shows better performance across a wider pH range. So, sugarcane bagasse biochar is more effective in this study.

Effect of Dose

The CV removal efficiency increased with adsorbent dose for both biochars (Fig. 3b). Rice straw biochar (RCB) removed only around 50% of CV at the lowest tested dose, but this rose to about 95–100% at the optimum dose of 0.7 g. Sugarcane bagasse biochar (SCB) showed a similar trend, reaching around 96% removal at its optimum dose of 0.4 g. Beyond these

doses, the removal plateaued, indicating saturation of available adsorption sites. Notably, SCB achieved high removal at a lower dose than RCB, reflecting its relatively higher adsorption efficiency per gram of material. SCB is more efficient due to its higher surface area and well-developed porous structure. It contains more oxygen-containing functional groups, enhancing dye binding. SCB has a higher cation exchange capacity, promoting electrostatic interactions with CV. Ibrahim et al., in 2020 found that increasing the dose of activated rice-straw biochar from 0.01 to 0.05 g raised CV removal from 29% to 95%, mirroring the positive dose–response seen here.

Effect of Initial Dye Concentration

Increasing the initial CV concentration led to a decrease in removal percentage for both biochars (Fig. 3c). RCB removed about 95% of CV at 40 mg/L but only around 90% at 100 mg/L, while SCB dropped from 96% to 93% over the same range. This drop in efficiency at higher dye loads is expected: with a fixed amount of adsorbent, more dye molecules must compete for the limited sites. Nevertheless, the removal remained high (>90%) even at 100 mg/L, indicating that both biochars have substantial capacity. This behavior is consistent with the literature. Ibrahim et al., in 2020 reported that increasing CV concentration reduced the percentage removal on rice-straw biochar, attributing it to active site limitation. Similarly, Hong Phuc et al., in 2025 found around 99.0% CV removal at 20 mg/L and 96.7% at 100 mg/L using a coffee-ground biochar. So, as initial dye concentration rises, removal (%) declines modestly due to saturation of adsorption sites, even though the absolute amount adsorbed increases.

Effect of Contact Time

The adsorption was rapid initially and reached equilibrium by 120 minutes for both biochars. In batch tests (Fig. 3d), the removal increased steeply during the first 60–120 min and then levelled off. By 120 min, both RCB and SCB had essentially saturated their adsorption sites, with RCB attaining slightly higher removal than SCB at earlier times (suggesting marginally faster kinetics). This faster initial uptake by RCB could be due to its pore structure or surface chemistry; for example, if RCB has smaller pore diameters or certain functional groups that bind CV more quickly, the initial adsorption rate would be higher. However, both biochars ultimately reach a similar high removal. The fact that SCB achieves higher capacity (q_m) but RCB has a slightly steeper initial uptake suggests that SCB's greater porosity and site density allow it to bind more dye overall, while RCB's surface properties enable rapid early adsorption. These results indicate that nearly all CV uptake occurs within the first two hours of contact. This time dependence agrees with other reports. Hong Phuc et al., in 2025 observed 89.3% CV removal in just 10 min and 96.5% by 60 min on a coffee-ground biochar. Likewise, Ashour et al., in 2022 found 88% removal in 15 min and equilibrium by 120 min for CV adsorbent. Thus, our biochars show typical adsorption kinetics, a rapid initial phase followed by saturation, similar to many other agricultural-waste-derived sorbents.

Adsorption isotherm

Fig. 4 and Table 1 showed the results of isotherm study. According to the Langmuir isotherm model, there are only a limited number of identical sites on a homogeneous surface where adsorption takes place. For rice straw biochar, the q_m value is 161.29 mg/g, with a Langmuir constant (K_l) of 7.91×10^{-4} L/mg and an R^2 value of 0.9838, indicating a good fit and high adsorption capacity. This reflects the effective utilization of adsorption sites at lower concentrations. With a K_l of 3.12×10^{-4} L/mg and an R^2 value of 0.9926, sugarcane bagasse biochar has a much larger q_m at 476.2 mg/g, indicating a somewhat lower affinity but still a greater adsorption capacity. Because sugarcane bagasse biochar has a bigger surface area and more adsorption sites, it performs better as seen by its higher q_{max}.

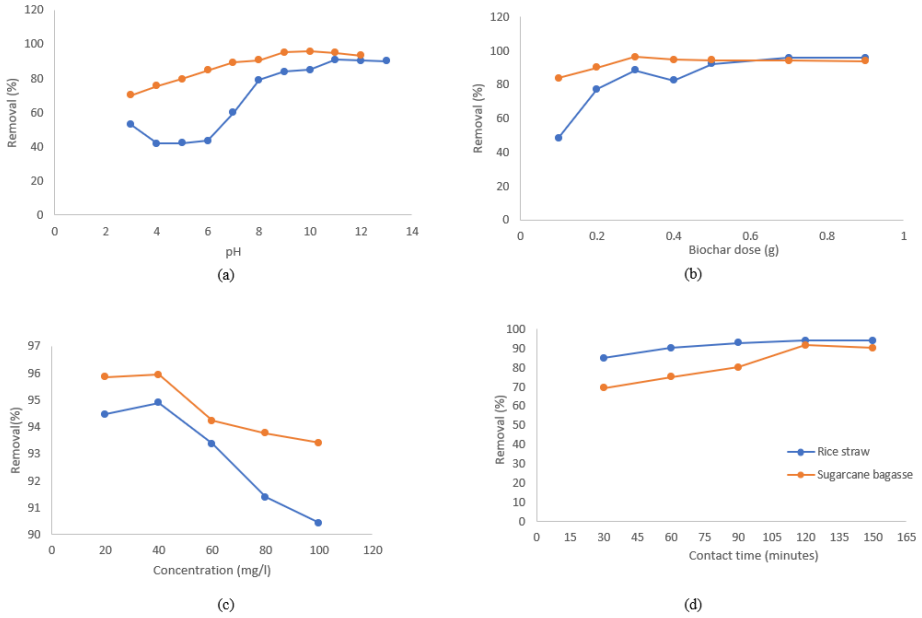

Fig. 4. Effect of (a) pH, (b) Biochar dose, (c) Initial Dye Concentration, and (d) Contact time on adsorption process

Table 1. Parameters of adsorption isotherm models for removal of crystal violet dye by bio-adsorbent

Model	Parameter	Rice Straw Biochar	Sugarcane Bagasse Biochar
Langmuir	q_m(mg/g)	161.29	476.2
	K_l (L/mg)	7.91×10^{-4}	3.12×10^{-4}
	R^2	0.9838	0.9926
Freundlich	n	1.4	1.16
	K_f (mg/g)	2.205	2.225
	R^2	0.9939	0.9985
Temkin	B(J/mol)	10.853	13.159
	K_t (L/g)	1.441	1.377
	R^2	0.9767	0.9637

Both biochars fit very well into the Freundlich isotherm model, best fit in this study, which postulates adsorption on a heterogeneous surface with sites of different affinities; the rice straw biochar has an R^2 value of 0.9939, while the sugarcane bagasse biochar has a value of 0.9985. The adsorption capabilities on heterogeneous surfaces of rice straw biochar and sugarcane bagasse biochar are similar, as indicated by their respective Freundlich constants (K_f) of 2.205 mg/g and 2.225 mg/g. For both biochars, the n values are more than 1, 1.4 for rice straw and 1.16 for sugarcane bagasse biochar, showing favourable adsorption conditions and increasing adsorption intensity at higher concentrations.The Temkin isotherm analysis yielded moderate correlations for both adsorbents. These B values indicate moderate adsorption heats and are consistent with the Temkin assumption that adsorbate–adsorbate interactions lead to a roughly linear decrease in adsorption energy as surface coverage increases, suggesting that heterogeneous surface adsorption dominates the behaviour. A higher K_t value indicates a stronger binding interaction between the dye and the surface, so the slightly larger K_t for RSB implies that it binds crystal violet marginally more strongly than SCB. The Freundlich isotherm provided the best overall

fit, followed closely by Langmuir. In summary, while Freundlich best describes the equilibrium data, the Temkin constants highlight that the heat of adsorption decreases approximately linearly with coverage, consistent with moderate adsorbate interactions observed in this system. Recent studies of CV removal on biochars often find the Freundlich isotherm provides the best fit. For example, biochars from coffee grounds (Hong Phuc et al., 2025b) and sugarcane bagasse (Mahdi et al., 2023) both showed Freundlich R^2 around 0.99, with exponent n >1 indicating favourable, multilayer adsorption.

Adsorption Kinetics

The processes controlling the adsorption process of crystal violet dye onto rice straw and sugarcane bagasse biochars are thoroughly understood thanks to the adsorption kinetics data (Fig. 5, Table 2). Lower R^2 values for the pseudo-first-order kinetic model (0.8487 for rice straw and 0.8951 for sugarcane bagasse) indicate that it is not as well suited to describe the adsorption process. The rate constants (k_1) are low, indicating a slower initial adsorption rate. Conversely, the pseudo-second-order kinetic model provides a much better fit with R^2 values of 0.9917 for rice straw and 0.9907 for sugarcane bagasse biochar, indicating that the adsorption process is likely governed by chemisorption involving valence forces through sharing or exchange of electrons between adsorbent and adsorbate. The higher rate constants (k_2) for sugarcane bagasse biochar (17.4 g/mg/min) compared to rice straw biochar (8.29 g/mg/min) reflect a faster adsorption process for sugarcane bagasse biochar.

The adsorption mechanism is further elucidated by the intraparticle diffusion model, with rice straw biochar exhibiting a value of 0.884 and sugarcane bagasse biochar exhibiting a value of 0.9264. This indicates the significance of intraparticle diffusion in the adsorption process. The higher K_{id} value of rice straw biochar (0.3374 mg/g/min$^{1/2}$) compared to sugarcane bagasse biochar (0.2302 mg/g/min$^{1/2}$) suggests a faster diffusion rate. Additionally, the sugarcane bagasse biochar has a higher intercept value (3.3048) than rice straw biochar (1.3898) which shows a stronger boundary layer influence during the adsorption process. The result shows that both

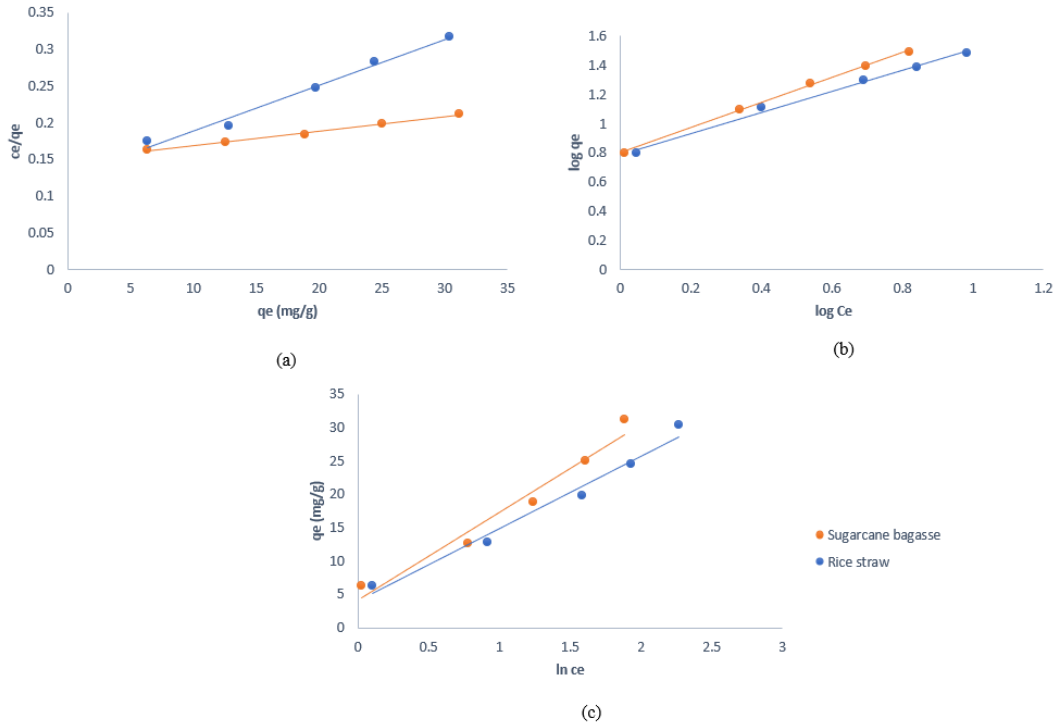

Fig. 5. (a) Langmuir isotherm, (b) Freundlich isotherm, (c) Temkin isotherm study adsorption of crystal violet dye on agro-residues.

Table 2. Parameters of adsorption kinetic models for removal of crystal violet dye by bio-adsorbent

Model	Parameter	Rice Straw Biochar	Sugarcane Bagasse Biochar
Pseudo-First-Order	k_1 (1/min)	0.0024	0.0066
	q_e (mg/g)	1.9955	3.61
	R^2	0.8487	0.8951
Pseudo-Second-Order	k_2 (g/mg/min)	8.29	17.4
	q_e (mg/g)	6.44	6.72
	R^2	0.9917	0.9907
Intraparticle Diffusion	K_{id} (mg/g/min$^{1/2}$)	0.3374	0.2302
	C	1.3898	3.3048
	R^2	0.884	0.9264

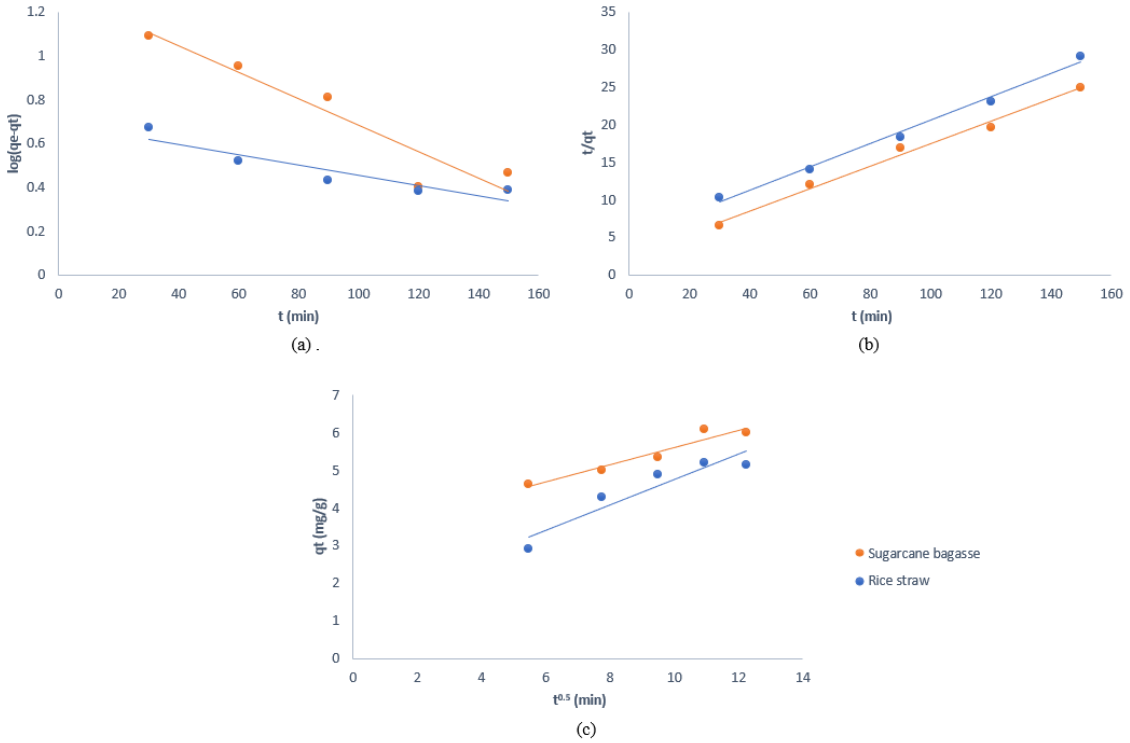

Fig. 6. Adsorption Kinetics of SCB and RSB; (a) Pseudo-first order, (b) Pseudo-second order, (c) Intraparticle diffusion model.

surface adsorption and intraparticle diffusion mechanisms take place, and sugarcane bagasse biochar has a more complex adsorption process which is particularly influenced by boundary layer diffusion. In studies of crystal-violet adsorption on biochars, the pseudo-second-order (PSO) model almost invariably provides the best fit ($R^2 \approx 0.99–1.00$), reflecting chemisorption-controlled kinetics. For example, (Mahdi et al., 2023) found that PSO fitting of CV uptake on sugarcane-bagasse biochars at 500 and 650 °C gave $R^2 = 1.000$ and 0.9998, respectively. Likewise, (Moharm et al., 2022) report $R^2 \approx 0.999$ for PSO (CV) versus only 0.888 for pseudo-first-order, with a PSO rate constant $k_2 \approx 1.2 \times 10^{-2}$ g/mg/min. In both cases the calculated q_e (PSO) closely matches experiment, which these authors interpret as a chemisorption-driven rate. Importantly, these works also find that intra-particle diffusion contributes significantly as

Table 3. Comparative study of adsorption of crystal violet dye by different bio-adsorbent.

Biochar Material	pH	Dose (g/l)	Dye concentration (mg/l)	Contact time (min)	Maximum adsorption capacity (mg/g)	Maximum Removal efficiency (%)	Isotherm models	Kinetics model	References
Modified rice husk	10 (1-12)	0.025 (0.01-0.06)	1000(10-1000)	70 (10-180)	90.02	96.16	LI*, FI	PSO	Homagai et al., 2022
Banana peel powder	7 (1-12)	1 (1-10)	90 (5-110)	10 (5-120)	-	93	LI*, FI, D-R	PFI*, PSO	Azhar-ul-Haq et al., 2024
Eucalyptus wood biomass	9 (2-10)	0.03 (0.02-0.10)	100	720 (5-700)	469.5	99.86	LI*,FI, D-R	PFO, PSO*	Yang et al., 2024
Platanus orientalis leaf powder	6.25 (2.62-6.52)	2.5 (0.5-3)	20 (5-40)	30 (5-60)	30.01	>90	LI, FI	PFO, PSO*	Ahmad Khan et al., 2023
Aerca leaf plate waste	8 (3-10)	3 (1-10)	50 (10-200)	-	-	87.44	LI*, FI, R-P, SI	PFO, PSO*	Nithyalakshmi & Saraswathi, 2023a
Sugarcane leaves	9 (2-11)	4.5 (0.5-5)	100 (100-700)	60 (10-100)	149.25	99.81	LI*,	PFO, PSO*	Patil et al., 2022
Sugarcane bagasse	9 (3-12)	4 (1-10)	40 (20-100)	120 (30-150)	476.2	>90	LI, FI*, TI	PFO, PSO*, IPD	Current study
Rice straw	11 (3-12)	7 (1-10)	40 (20-100)	120 (30-120)	161.29	>90	LI, FI*, TI	PFO, PSO*, IPD	

* Represents best fit model in the study

they observed a two-stage uptake (fast surface binding followed by slower pore diffusion) with an intraparticle-diffusion fit of $R^2 \approx 0.905$.

Comparison with Previous Crystal Violet Adsorption Studies

Table 3 summarizes recent CV adsorption on various biochars under their respective experimental conditions. Homagai et al. (2022) prepared xanthated rice husk (XRH) and conducted adsorption at pH 10, 25 °C, initial (CV) = 50 mg/ L, 0.25 g L^{-1} adsorbent, and 60 min contact, yielding q_m = 90.02 mg g^{-1}. Azhar-ul-Haq et al. (2024) used raw banana peel powder at pH 7, 20 °C, initial (CV) = 90 mg L^{-1}, 1 g adsorbent, and 10 min contact, achieving 93 % removal. Yang et al. (2024) synthesized succinic-anhydride–modified eucalyptus biochar at pH 9, 25 °C, initial (CV) = 100 mg L^{-1}, 0.3 g L^{-1} adsorbent—finding q_m = 469.5 mg g^{-1}. Patil et al. (2022) prepared microwave and acid-activated sugarcane leaf char, operating at pH 9, 25 °C, initial (CV) = 100 mg L^{-1}, 4.5 g L^{-1} adsorbent, and 60 min contact, with q_m = 149.25 mg g^{-1}. In our present work, unactivated rice straw biochar (550 °C pyrolysis) at pH 11, 25 °C, initial (CV) = 40 mg L^{-1}, 7 g L^{-1} adsorbent, 120 min contact shows q_m = 161.29 mg g^{-1}, whereas unactivated sugarcane bagasse biochar (550 °C) at pH 9, 25 °C, initial [CV] = 40 mg L^{-1}, 4 g L^{-1} adsorbent, 120 min contact yields q_m = 476.2 mg g^{-1}. This comparison shows that despite similar feedstocks, surface chemistry and operating conditions drastically affect adsorption capacity for CV. The literature shows that dye uptake on biochars is generally driven by a few recurring processes. In almost all cases studied, cationic or anionic dyes are attracted to oppositely-charged sites on the biochar surface via strong electrostatic interaction, while aromatic dyes also engage in π–π (and n–π) stacking with the biochar's graphitic or aromatic domains. At the same time, polar surface functional groups (–OH, –COOH, –NH2, etc.) form

hydrogen bonds or dipole interactions with complementary groups on the dye.

CONCLUSION

The study found that the optimal conditions for the adsorption of crystal violet dye using biochars derived from rice straw and sugarcane bagasse included a pH of 11 for rice straw biochar and 9 for sugarcane bagasse biochar, a biochar dose of 7 g/l for rice straw and 4 g/l for sugarcane bagasse, an initial dye concentration of 40 mg/L for both biochars, and an optimal contact time of 120 minutes. While these pH values are higher than those typically found in real wastewater (pH 6.5–8.5), they represent the maximum adsorption capacity under ideal conditions. Further optimization or surface modification may enhance performance under natural pH conditions. The data fitted the Freundlich isotherm best ($R^2 = 0.9939$ for rice straw; $R^2 = 0.9985$ for sugarcane bagasse), indicating multilayer adsorption on heterogeneous surfaces and favourable adsorption intensity ($n > 1$). While the Freundlich model gave the best fit, the Langmuir model also showed high correlation, suggesting the presence of monolayer adsorption at specific homogeneous sites, and the Temkin model indicated moderate adsorbate–adsorbate interactions through its linear decrease in adsorption energy. The most suitable kinetic model for the adsorption process was pseudo-second order, implying that the rate-limiting step likely involves valence forces through electron sharing or exchange in a chemisorption process. These results demonstrate that both biochars have promising potential for dye removal in wastewater treatment under optimized conditions. Furthermore, they are relatively practical and applicable, offering environmentally friendly disposal options and potential reuse in agricultural applications, such as soil amendment or nutrient retention.

AUTHOR'S CONTRIBUTION

Meenakshi Nandal: Conceptualization, methodology, Data curation, validation and reviewing; Jyoti chowdhry: Experiment performing, writing original draft, software; Khush Kataria: Software, Statistical modelling, Model interpretation; Pradeep Khyalia: Methodology, data curation, Statistical analysis, draft editing, reviewing; Jitender Singh Laura: Data curation, reviewing, validation.

DECLARATION OF INTERESTS

The authors declare that they have no known competing financial interests or personal relationships that could have appeared to influence the work reported in this paper.

LIFE SCIENCE REPORTING

No life science threat was practiced in this research.

FUNDING INFORMATION

No funding was received for this research.

DATA AVAILABILITY

Data can be make available on reasonable request.

REFERENCES

Abd-Elhamid, A. I., Emran, M., El-Sadek, M. H., El-Shanshory, A. A., Soliman, H. M., Akl, M. A., & Rashad, M. (2020). Enhanced removal of cationic dye by eco-friendly activated biochar derived from rice straw. *Applied Water Science*, 10; 1-11.

Abu Elella, M. H., Sabaa, M. W., ElHafeez, E. A., & Mohamed, R. R. (2019). Crystal violet dye removal using crosslinked grafted xanthan gum. *International Journal of Biological Macromolecules*, 137; 1086-1101.

Ahmad Khan, F., Ahad, A., Shah, S. S., & Farooqui, M. (2023). Adsorption of crystal violet dye using Platanus orientalis (Chinar tree) leaf powder and its biochar: Equilibrium, kinetics and thermodynamics study. *International Journal of Environmental Analytical Chemistry*, 103(16); 4820–4840.

APHA. *Standard Methods for the Examination of Water and Wastewater*; American Public Health Association: Washington, DC, USA, 1995.

Arivumani, V., Singh, V., Geetha, C., & Senthilkumar, C. (2024). Activated rice husk biochar for azo dye removal: Batch adsorption, kinetics and thermodynamic studies. *Global NEST Journal*, 26(2); 05498.

Azhar-ul-Haq, M., Javed, T., Abid, M. A., Masood, H. T., & Muslim, N. (2024). Adsorptive removal of hazardous crystal violet dye onto banana peel powder: equilibrium, kinetic and thermodynamic studies. *Journal of Dispersion Science and Technology*, 45(3); 475-490.

Barría, Y., Burbano, A., James, A., Gascó, G., & Méndez, A. (2023). Sorption capacity of biochars obtained by gasification of rice husks and wild sugarcane: Removal of malachite green and arsenic from water solutions. *Biomass Conversion and Biorefinery*, 15; 2131–2143.

Bhatti, H. N., Sadaf, S., Naz, M., Iqbal, M., Safa, Y., Ain, H. U., ... & Nazir, A. (2021). Enhanced adsorption of Foron Black RD 3GRN dye onto sugarcane bagasse biomass and Na-alginate composite. *Desalination Water Treat*, 216; 423-435.

Cao, D., Wang, J., Zhang, Q., Wen, Y., Dong, B., Liu, R., Yang, X., & Geng, G. (2019). Biodegradation of triphenylmethane dye crystal violet by Cedecea davisae. *Spectrochimica Acta Part A: Molecular and Biomolecular Spectroscopy*, 210; 9-13.

Chahinez, H. O., Abdelkader, O., Leila, Y., & Tran, H. N. (2020). One-stage preparation of palm petiole-derived biochar: Characterization and application for adsorption of crystal violet dye in water. *Environmental Technology & Innovation*, 19; 100872.

Chen, X., Lin, Q., He, R., Zhao, X., & Li, G. (2017). Hydrochar production from watermelon peel by hydrothermal carbonization. *Bioresource technology*, 241; 236-243.

Conceição, F., Moruzzi, R., Duarte, G., Galileu Speranza, L., Antunes, M., & Mancini, S. (2022). Biochar from sugarcane bagasse for reactive dye adsorption considering a circular economy approach. *Journal of Textile Engineering & Fashion Technology*, 8, 126–132.

Foong, S. Y., Chan, Y. H., Chin, B. L. F., Lock, S. S. M., Yee, C. Y., Yiin, C. L., ... & Lam, S. S. (2022). Production of biochar from rice straw and its application for wastewater remediation− An overview. *Bioresource Technology*, 127588.

Geetha, T., Smitha, J. K., Sebastian, M., Litty, M. I., Joseph, B., Joseph, J., & Nisha, T. S. (2024). Synthesis and characterization of nano iron oxide biochar composite for efficient removal of crystal violet from water. *Heliyon*, 10(21); e39450

Gonçalves, J. O., Crispim, M. M., Rios, E. C., Silva, L. F., de Farias, B. S., Sant'Anna Cadaval Junior, T. R., ... & Dotto, G. L. (2024). New and effective cassava bagasse–modified biochar to adsorb Food Red 17 and Acid Blue 9 dyes in a binary mixture. *Environmental Science and Pollution Research*, 31(4); 5209-5220.

Hazzaa, R., & Hussein, M. (2015). Cationic dye removal by sugarcane bagasse activated carbon from aqueous solution. *Global NEST Journal*, 17(4); 784-795.

Hussein, T. K., & Jasim, N. A. (2019). Removal of crystal violet and methylene blue from synthetic industrial wastewater using fennel seed as an adsorbent. *Journal of Engineering Science and Technology*, 14(5); 2947-2963.

Homagai, P. L., Poudel, R., Poudel, S., & Bhattarai, A. (2022). Adsorption and removal of crystal violet dye from aqueous solution by modified rice husk. *Heliyon*, 8(4); e09261.

Jabeen, A., & Bhatti, H. N. (2021). Adsorptive removal of reactive green 5 (RG-5) and direct yellow 50 (DY-50) from simulated wastewater by Mangifera indica seed shell and its magnetic composite: Batch and Column study. *Environmental Technology & Innovation*, 23; 101685.

Jais, F. M., Ibrahim, S., Chee, C. Y., & Ismail, Z. (2021). High removal of crystal violet dye and tetracycline by hydrochloric acid assisted hydrothermal carbonization of sugarcane bagasse prepared at high yield. *Sustainable Chemistry and Pharmacy*, 24; 100541.

Kamal, M. A., Bibi, S., Bokhari, S. W., Siddique, A. H., & Yasin, T. (2017). Synthesis and adsorptive characteristics of novel chitosan/graphene oxide nanocomposite for dye uptake. *Reactive and Functional Polymers*, 110; 21-29.

Khan, S., Ahamad, Z., & Nasar, A. (2023). Development and utilization of raw and NaOH-modified peanut hull as potential adsorbents for crystal violet dye removal from wastewater. *Biomass Conversion and Biorefinery*, 1-21.

Khoramzadeh, E., Nasernejad, B., & Halladj, R. (2013). Mercury biosorption from aqueous solutions by sugarcane bagasse. *Journal of the Taiwan Institute of Chemical Engineers*, 44(2); 266-269.

Kumar, A., Kumar, V., & Singh, B. (2021). Cellulosic and hemicellulosic fractions of sugarcane bagasse: Potential, challenges and future perspective. *International Journal of Biological Macromolecules*, 169; 564-582.

Kyi, P. P., Quansah, J. O., Lee, C. G., Moon, J. K., & Park, S. J. (2020). The removal of crystal violet from textile wastewater using palm kernel shell-derived biochar. *Applied Sciences*, 10(7); 2251.

Lellis, B., Fávaro-Polonio, C. Z., Pamphile, J. A., & Polonio, J. C. (2019). Effects of textile dyes on health and the environment and bioremediation potential of living organisms. *Biotechnology Research and Innovation*, 3(2); 275-290.

Li, X., Li, M. F., Bian, J., Wang, B., Xu, J. K., & Sun, R. C. (2015). Hydrothermal carbonization of bamboo in an oxalic acid solution: effects of acid concentration and retention time on the characteristics of products. *RSC advances*, 5(94); 77147-77153.

Luyen, N. T., Linh, H. X., & Huy, T. Q. (2020). Preparation of rice husk biochar-based magnetic nanocomposite for effective removal of crystal violet. *Journal of Electronic Materials*, 49(2); 1142-1149.

Maurya, D. P., Singla, A., & Negi, S. (2015). An overview of key pretreatment processes for biological conversion of lignocellulosic biomass to bioethanol. *3 Biotech*, 5; 597-609.

Moharm, A. E., El Naeem, G. A., Soliman, H. M., I., A., A., A., Kassem, T. S., Nayl, A. A., & Bräse, S. (2021). Fabrication and Characterization of Effective Biochar Biosorbent Derived from Agricultural Waste to Remove Cationic Dyes from Wastewater. *Polymers*, 14(13); 2587.

Nithyalakshmi, B., & Saraswathi, R. (2023a). Removal of colorants from wastewater using biochar derived from leaf waste. *Biomass Conversion and Biorefinery*, 1-17.

Nithyalakshmi, B., Saraswathi, R., & Praveen, S. (2023b). Removal of basic fuchsin red dye by turmeric leaf waste biochar: Batch adsorption studies, isotherm kinetics and RSM studies. *Global Nest Journal*, 25(1); 17-27.

Patil, S. A., Kumbhar, P. D., Satvekar, B. S., Harale, N. S., Bhise, S. C., Patil, S. K., ... & Anuse, M. A. (2022). Adsorption of toxic crystal violet dye from aqueous solution by using waste sugarcane leaf-based activated carbon: isotherm, kinetic and thermodynamic study. *Journal of the Iranian Chemical Society*, 19(7); 2891-2906.

Peng, X. Y. L. L., Ye, L. L., Wang, C. H., Zhou, H., & Sun, B. (2011). Temperature-and duration-dependent rice straw-derived biochar: Characteristics and its effects on soil properties of an Ultisol in southern China. *Soil and tillage research*, 112(2); 159-166.

Rápó, E., & Tonk, S. (2020). Factors Affecting Synthetic Dye Adsorption; Desorption Studies: A Review of Results from the Last Five Years (2017–2021). *Molecules*, 26(17); 5419.

Sackey, E. A., Song, Y., Yu, Y., & Zhuang, H. (2021). Biochars derived from bamboo and rice straw for sorption of basic red dyes. *PLoS One*, 16(7); e0254637.

Sahoo, J. K., Hota, A., Singh, C., Barik, S., Sahu, N., Sahoo, S. K., ... & Sahoo, H. (2023). Rice husk and rice straw based materials for toxic metals and dyes removal: A comprehensive and critical review. *International Journal of Environmental Analytical Chemistry*, 103(20); 9131-9153.

Salah omer, A., A.El Naeem, G., Abd-Elhamid, A., O.M. Farahat, O., A. El-Bardan, A., M.A. Soliman, H., & Nayl, A. (2022). Adsorption of crystal violet and methylene blue dyes using a cellulose-based adsorbent from sugercane bagasse: Characterization, kinetic and isotherm studies. *Journal of Materials Research and Technology*, 19; 3241-3254.

Salahudeen, N., & Rasheed, A. A. (2020). Kinetics and thermodynamics of hydrolysis of crystal violet at ambient and below ambient temperatures. *Scientific Reports*, 10(1); 1-9.

Shin, J., Kwak, J., Lee, Y. G., Kim, S., Choi, M., Bae, S., ... & Chon, K. (2021). Competitive adsorption

of pharmaceuticals in lake water and wastewater effluent by pristine and NaOH-activated biochars from spent coffee wastes: Contribution of hydrophobic and π-π interactions. *Environmental Pollution*, 270; 116244.

Wathukarage, A., Herath, I., Iqbal, M. C. M., & Vithanage, M. (2019). Mechanistic understanding of crystal violet dye sorption by woody biochar: implications for wastewater treatment. *Environmental geochemistry and health*, 41; 1647-1661.

Yang, P., Lu, Y., Zhang, H., Li, R., Hu, X., Shahab, A., Elnaggar, A. Y., Alrefaei, A. F., AlmutairiI, M. H., & Ali, E. (2024). Effective removal of methylene blue and crystal violet by low-cost biomass derived from eucalyptus: Characterization, experiments, and mechanism investigation. *Environmental Technology & Innovation*, 33; 103459.

Zafeer, M. K., Menezes, R. A., Venkatachalam, H., & Bhat, K. S. (2024). Sugarcane bagasse-based biochar and its potential applications: a review. *Emergent Materials*, 7(1); 133-161.

Zhang, H., Xue, G., Chen, H., & Li, X. (2018). Magnetic biochar catalyst derived from biological sludge and ferric sludge using hydrothermal carbonization: preparation, characterization and its circulation in Fenton process for dyeing wastewater treatment. *Chemosphere*, 191; 64-71.

Zhao, Y., Li, W., Zhao, X., Wang, D. P., & Liu, S. X. (2013). Carbon spheres obtained via citric acid catalysed hydrothermal carbonisation of cellulose. *Materials Research Innovations*, 17(7); 546-551.